

## DUST OBSCURATION IN LYMAN BREAK GALAXIES AT $z \sim 4$

I-TING HO<sup>1</sup>, WEI-HAO WANG<sup>1</sup>, GLENN E. MORRISON<sup>2,3</sup>, AND NEAL A. MILLER<sup>4</sup>

*ApJ accepted, August 2010*

### ABSTRACT

Measuring star formation rates (SFRs) in high- $z$  galaxies with their rest-frame ultraviolet (UV) continuum can be uncertain because of dust obscuration. Prior studies had used the submillimeter emission at  $850 \mu\text{m}$  to determine the intrinsic SFRs of rest-frame UV selected galaxies, but the results suffered from the low sensitivity and poor resolution ( $\sim 15''$ ). Here, we use ultradeep Very Large Array 1.4 GHz images with  $\sim 1''$ – $2''$  resolutions to measure the intrinsic SFRs. We perform stacking analyses in the radio images centered on  $\sim 3500$  Lyman break galaxies (LBGs) at  $z \sim 4$  in the Great Observatories Origins Deep Survey-North and South fields selected with *Hubble Space Telescope*/Advanced Camera for Surveys data. The stacked radio flux is very low,  $0.08 \pm 0.15 \mu\text{Jy}$ , implying a mean SFR of  $6 \pm 11 M_{\odot} \text{yr}^{-1}$ . This is comparable to the uncorrected mean UV SFRs of  $\sim 5 M_{\odot} \text{yr}^{-1}$ , implying that the  $z \sim 4$  LBGs have little dust extinction. The low SFR and dust extinction support the previous results that  $z \sim 4$  LBGs are in general not submillimeter galaxies. We further show that there is no statistically significant excess of dust-hidden star-forming components within  $\sim 22$  kpc from the LBGs.

*Subject headings:* dust, extinction — galaxies: evolution — galaxies: high-redshift — radio continuum: galaxies

### 1. INTRODUCTION

Understanding galaxy evolution in the early Universe requires large samples of various kinds of high- $z$  galaxies. One important technique enabling selections of  $z > 2.5$  star-forming galaxies is the Lyman break technique (Cowie et al. 1988; Songaila et al. 1990; Lilly et al. 1991; Steidel & Hamilton 1993; Steidel et al. 1995; also see a review in Giavalisco 2002). The UltraViolet (UV) spectrum of a high-redshift star-forming galaxy usually exhibits a Lyman continuum discontinuity at  $912 \text{ \AA}$ , which is caused by absorption of H I in the stellar atmosphere of massive stars, and interstellar and intergalactic media. By using this feature, large samples of Lyman break galaxies (LBGs) can be selected in various redshift ranges by searching for sudden brightness dropouts between two adjacent broad-band images.

An important property of LBGs is their star formation rates (SFRs). However, determining SFRs for  $z > 3$  systems is still challenging because most of the diagnostics at low redshifts are unavailable when light becomes dimmer and redshifts to wavelengths that are harder to observe. One of the most commonly used method to determine SFRs at high redshift is to measure the rest-frame UV continuum which shifts at  $z > 3$  to the optical and near-infrared (e.g., Kennicutt 1998). Unfortunately, the UV continuum can be easily attenuated by dust, which results in underestimation of the SFRs. Bouwens et al. (2009) attempted to determine the correction factor by using the observed correlation between the ratio of far-infrared (FIR) to UV flux and the UV spectral slope (Meurer et al. 1999). They found that UV continuum of  $z \sim 4$  LBGs in the Great Observatories Origins Deep Survey-North (GOODS-N)

and South (GOODS-S) fields underestimates SFRs by factors of  $\sim 3$ – $6$ . However, this result is debatable since the correlation exhibits significant scatter in different populations of galaxies (e.g., Cortese et al. 2006; Howell et al. 2010).

A more direct way to estimate the SFRs is to deduce them at longer wavelengths where light is not affected by dust obscuration. Efforts had been made using the submillimeter  $850 \mu\text{m}$  emission to determine the intrinsic SFRs in LBGs (Peacock et al. 2000; Chapman et al. 2000; Webb et al. 2003). However, these results have low signal-to-noise ratios (S/Ns), presumably because the submillimeter single-dish maps were not deep enough, a consequence of instrumental, sky, and confusion noises (i.e., uncertainties contributed by nearby bright sources or faint undetected sources). In addition, an assumption of dust temperature is required to estimate the total infrared (IR) luminosity. These all make the estimate of SFRs based on submillimeter measurements quite uncertain.

The radio wavelength is an alternative probe of SFRs. At 1.4 GHz, the radio continuum is dominated by synchrotron radiation from relativistic electrons produced by supernovae. By converting the 1.4 GHz luminosity to total IR luminosity with the well-known radio—FIR correlation (Condon 1992), it is possible to estimate intrinsic SFRs (Kennicutt 1998). The radio—FIR correlation is fairly insensitive to dust temperature. The angular resolution in the radio can be very high ( $\sim 1''$ – $2''$ ), meaning very little confusion noise. Because of these great advantages, this radio-based method has been used in various high- $z$  studies (e.g., Reddy & Steidel 2004; Wang et al. 2006; Carilli et al. 2008; Pannella et al. 2009).

The Very Large Array (VLA) provides high resolution in the radio, but its sensitivity is insufficient for directly detecting normal star-forming galaxies at  $z \gtrsim 1.5$ . Therefore, stacking radio fluxes of large samples of LBGs to determine their mean SFRs is a necessary approach. Reddy & Steidel (2004) stacked  $z \sim 2$  LBGs and found the dust correction to be  $\sim 4.5$ . Using a similar method, Carilli et al. (2008) determined the dust correction for  $z \sim 3$  LBGs to be 1.8.

In order to determine the intrinsic SFRs for  $z \sim 4$  LBGs,

itho@ifa.hawaii.edu; itho@asiaa.sinica.edu.tw

<sup>1</sup> Institute of Astronomy & Astrophysics, Academia Sinica, P.O. Box 23-141, Taipei 10617, Taiwan

<sup>2</sup> Institute for Astronomy, University of Hawaii, Honolulu, HI 96822, USA

<sup>3</sup> Canada-France-Hawaii Telescope, Kamuela, HI 96743, USA

<sup>4</sup> Department of Astronomy, University of Maryland, College Park, MD 20742, USA

we performed radio stacking analyses in the GOODS-N and GOODS-S fields. The GOODS *Hubble Space Telescope/Advance Camera for Surveys (HST/ACS)* data (Giavalisco et al. 2004) were used to locate  $\sim 3500$  LBGs in the fields, and deep VLA 1.4 GHz images (Miller et al. 2008; Morrison et al. 2010) were used to measure and stack the radio fluxes. We note that although radio stacking of  $z \sim 4$  LBGs had also been attempted by Carilli et al. (2008), we used much deeper optical images ( $\sim 2$  mag deeper at  $V$  band) and radio images ( $\sim 15\% - 40\%$  deeper). We are therefore probing much closer to the typical members in the  $z \sim 4$  LBG population, as in Bouwens et al. (2009).

In this paper, we first describe the observational data in Section 2. In Section 3, we describe our methods of selecting LBGs, stacking analysis, and estimations of SFRs using radio and UV. Finally, we compare the two different SFRs and discuss the implications in Section 4, and give a summary in Section 5. We assume  $\Omega_0 = 0.3$ ,  $\Omega_\Lambda = 0.7$ , and  $H_0 = 70 \text{ km s}^{-1} \text{ Mpc}^{-1}$ . All magnitudes are in the AB magnitude system.

## 2. DATA

### 2.1. HST/ACS

The *HST/ACS* multiband imaging in the GOODS fields (Giavalisco et al. 2004) consists of four passbands: F435W, F606W, F775W, and F850LP, which are referred to as  $B_{435}$ ,  $V_{606}$ ,  $i_{775}$ , and  $z_{850}$ , respectively. We adopt the v2.0 source catalogs for selecting our LBG samples. Quantities measured with SExtractor (Bertin & Arnouts 1996) “automatic aperture” (MAG\_AUTO, FLUX\_AUTO, etc.) are used to approximate total values.

### 2.2. VLA

The VLA 1.4 GHz images of the GOODS-N and GOODS-S fields are described in more details in Morrison et al. (2010) and Miller et al. (2008), respectively. In brief, the North field has an rms noise of  $\sim 4 \mu\text{Jy beam}^{-1}$  at the center, and  $< 6 \mu\text{Jy beam}^{-1}$  at the edges of the ACS fields. The South field has an rms noise of  $\sim 6 \mu\text{Jy beam}^{-1}$  at the center, and  $< 7.5 \mu\text{Jy beam}^{-1}$  at the edges of the fields. These sensitivities have been corrected for the primary beam response. The beam FWHM of the North field is  $1''.7 \times 1''.6$ , which corresponds to  $11.8 \text{ kpc} \times 11.1 \text{ kpc}$  at  $z = 4$ . The beam FWHM of the South field is  $2''.8 \times 1''.6$ , which corresponds to  $19.5 \text{ kpc} \times 11.1 \text{ kpc}$  at  $z = 4$ . Data Release 2 of the South field is used here.

## 3. METHOD

### 3.1. Sample Selection

“ $B$ -dropout” galaxies at  $z \sim 4$  are selected utilizing the redshifted Lyman break located between  $B_{435}$  and  $V_{606}$ . We adopt the well established criteria (e.g., Beckwith et al. 2006; Bouwens et al. 2007):

$$\begin{aligned} B_{435} - V_{606} &> 1.1, \\ B_{435} - V_{606} &> (V_{606} - z_{850}) + 1.1, \\ V_{606} - z_{850} &< 1.6, \\ S/N(V_{606}) &> 5, \text{ and } S/N(i_{775}) > 3. \end{aligned}$$

In addition, compact objects (SExtractor stellarity indices greater than 0.8) with  $i_{775} < 26.5$  are rejected from our sample to prevent stellar contamination. A color-color diagram

illustrating the sample selection is shown in Figure 1. In total, we selected 1778 and 1679  $B$ -dropouts in the North and South fields, respectively. These selection criteria efficiently select LBGs between  $z \sim 3$  and  $z \sim 4.5$ , with a mean redshift of 3.8 (see more details in Bouwens et al. 2007). The number of LBGs selected by us is very similar to that in Bouwens et al. (2007), who used similar GOODS ACS data.

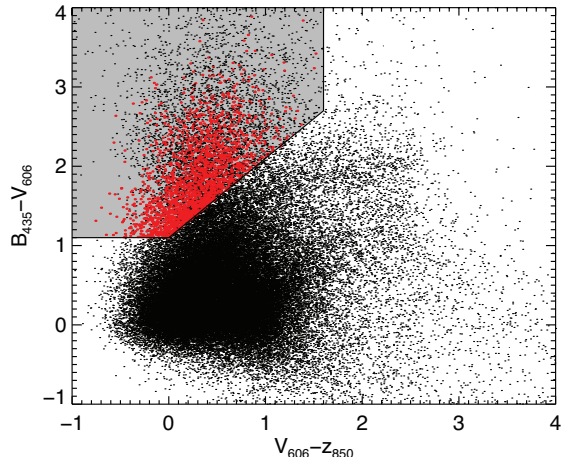


FIG. 1.— A color-color diagram showing the  $B$ -dropouts selection criteria. Objects in the GOODS fields are plotted with dots. Intersection of the three color selection criteria described in Section 3.1 are shaded in grey. The selected LBGs are shown with red dots. Note that some of the objects inside the grey region are not selected as LBGs because they do not meet the other criteria (e.g., low S/N or too compact).

### 3.2. Stacking Analyses

We measured the radio fluxes of the  $z \sim 4$  LBGs with aperture photometry at their optical positions. Small offsets ( $< 0''.3$ ) between the coordinates of the radio and optical images had been corrected utilizing their source catalogs. Apertures of two different sizes were used here: small-apertures with radii equal to the beam FWHMs ( $\sim 11 \text{ kpc}$  at  $z = 4$ ); large-apertures with radii equal to twice the beam FWHMs ( $\sim 22 \text{ kpc}$  at  $z = 4$ ). Here we first focus on the small aperture results and we will discuss the large aperture results in Section 4.4. Elliptical apertures were used for the South field to match its beam shape. Fluxes measured with our aperture photometry were calibrated with the radio catalogs (Miller et al. 2008; Morrison et al. 2010). For sources in the radio catalogs, we measured their fluxes with our aperture photometry and computed the median of the ratios between our fluxes and the catalog fluxes. The ratios, which were found to be very close to unity for the aperture sizes we used, were applied back to our radio fluxes.

Sources with radio fluxes  $> 100 \mu\text{Jy}$  were rejected from our measurements because their radio fluxes do not likely reflect their true SFRs. There are eight such sources. If they are normal star-forming galaxies at  $z = 4$ , their IR luminosity would be  $\gtrsim 5 \times 10^{13} L_\odot$  (or SFR  $\gtrsim 7000 M_\odot \text{ yr}^{-1}$ ), which is unusually large. We inspected these sources individually. They either are affected by nearby bright radio sources that do not appear to be at the same redshifts of the LBGs, or do not appear to be associated with known submillimeter galaxies (SMGs) in the samples of Wang et al. (2004), Perera et al. (2008), Devlin et al. (2009), and Weiß et al. (2009). Therefore, they are highly unlikely high-redshift ultraluminous starbursting galaxies. To avoid the bias from unrelated nearby

bright sources and from active galactic nuclei (AGNs), we did not include these eight sources in our stacking analyses. For those sources with radio fluxes  $< 100 \mu\text{Jy}$ , we then averaged their radio fluxes and subtracted a background value (see below) from the means to get the final stacked radio fluxes.

The uncertainties of our stacked fluxes were estimated with Monte Carlo simulations, with an assumption that the galaxies are distributed randomly over the map. We measured the mean radio fluxes at random positions, and the number of random positions is the same as that of the  $< 100 \mu\text{Jy}$   $B$ -dropouts. The same apertures were used and the same rejection criterion of  $< 100 \mu\text{Jy}$  was adopted. This measurement is repeated 10,000 times, and the mean radio fluxes have a fairly Gaussian-like distribution. We then calculated the mean and the dispersion of these 10,000 measurements. The mean was subtracted from the stacked radio flux of the LBG sample to form the final stacked radio flux. This subtraction is to account for the effect of imperfect clean and chance projection of random radio sources in our flux apertures. Likewise, the dispersion can then represent the uncertainty of the stacked radio flux.

There are two caveats in the above procedures. First, if  $z \sim 4$  LBGs are clustered at scales similar to the sizes of our apertures, our assumption that LBGs are randomly distributed would break down. Our stacking method would then overestimate the radio fluxes. We investigated clustering with the same method used by Marsden et al. (2009). We found that the variance-to-mean ratio of source numbers inside randomly placed  $r < 10''$  circles of our sample exceeds that of random distribution by less than 0.1, and becomes smaller with smaller radii. Therefore, we conclude that there is no significant small-scale clustering in our LBG sample and the flux overestimate caused by small-scale clustering can be neglected.

Second, the faulty estimate of uncertainties can be caused by concentration of sources in high or low sensitivity regions (i.e., the slightly uneven sensitivity distribution caused by the primary beam falloff in the GOODS-N or by the mosaicking in the GOODS-S). Instead of stacking at random positions to estimate the uncertainty, we also carried out the simulation based on the source positions of the real LBG sample. We added an offset to the positions of the LBGs and stacked their fluxes. We repeated this for 10,000 times with different random offsets of  $15'' - 60''$ , and calculated the mean and the dispersion. The results are within 30% to those measured from random positions, suggesting that LBGs are not concentrated in specific regions.

With the above methods, we measured the final stacked fluxes and flux errors of the LBGs in the two fields separately. For each aperture size, we combined the two final stacked fluxes by weighting them with the inverse of the square-errors to form the combined flux. The results are summarized in Table 1. The stacked radio signal is very weak, consistent with zero within the noise.

### 3.3. Star Formation Rate

#### 3.3.1. Radio SFR

The stacked radio fluxes can be converted to SFRs. Assuming a universal synchrotron emission spectral index of  $\alpha = -0.8$ , we convert the stacked radio fluxes  $S_{\text{stack}}$  to the rest-frame 1.4 GHz luminosity densities  $L_{1.4\text{GHz}}$ , i.e.,

$$L_{1.4\text{GHz}} = 4\pi d_l^2 S_{\text{stack}} (1+z)^{-(1+\alpha)}, \quad (1)$$

TABLE 1  
MEAN RADIO FLUXES

Field	Small Aperture <sup>a</sup>		Large Aperture <sup>b</sup>	
	$F_{\text{LBG}}$ ( $\mu\text{Jy}$ )	$F_{\text{random}}$ ( $\mu\text{Jy}$ )	$F_{\text{LBG}}$ ( $\mu\text{Jy}$ )	$F_{\text{random}}$ ( $\mu\text{Jy}$ )
GOODS-N	$-0.05 \pm 0.18$	$0.36 \pm 0.18$	$0.29 \pm 0.28$	$1.10 \pm 0.28$
GOODS-S	$0.36 \pm 0.26$	$0.10 \pm 0.26$	$0.54 \pm 0.54$	$-0.03 \pm 0.54$
Combined	$0.08 \pm 0.15$	-	$0.34 \pm 0.25$	-

NOTE. —  $F_{\text{random}}$  is the mean radio flux of random positions derived with the Monte Carlo simulation in Section 3.2. This mean is subtracted from the measured flux of the LBG sample, and its error is propagated to the mean of the LBG sample.  $F_{\text{LBG}}$  listed has already been subtracted by  $F_{\text{random}}$ .

<sup>a</sup>Apertures with radii equal to the beam FWHM.

<sup>b</sup>Apertures with radii equal to twice the beam FWHM.

where  $d_l$  is the luminosity distance and  $z$  is the mean redshift of 3.8. With the local radio—FIR correlation (Helou et al. 1985; Condon 1992),  $L_{1.4\text{GHz}}$  can be converted to FIR luminosity  $L_{\text{FIR}(40-120)}$ , approximately the total luminosity between  $\lambda = 42.5 \mu\text{m}$  and  $\lambda = 122.5 \mu\text{m}$ , with the following relation:

$$q = \log \frac{L_{\text{FIR}(40-120)}}{3.75 \times 10^{12} \text{ W}} - \log \frac{L_{1.4\text{GHz}}}{\text{W Hz}^{-1}}, \quad (2)$$

with  $q = 2.34 \pm 0.01$  (Yun et al. 2001). Although this value was derived locally ( $z \lesssim 0.15$ ), recent studies suggest weak evolution out to  $z \sim 2$  (Sargent et al. 2010; Ivison et al. 2010a,b). Extrapolating  $q$  to  $z = 4$  using the relation  $q \propto (1+z)^\gamma$  with  $\gamma = -0.04 \pm 0.03$  (Ivison et al. 2010b) implies that  $L_{\text{FIR}}$  (and therefore radio SFRs) will be lowered by only  $\sim 30\% \pm 20\%$ , which is insignificant compared to the uncertainties in our results.

SFRs can then be estimated with the conversion in Kennicutt (1998):

$$\frac{\text{SFR}}{(\text{M}_\odot \text{ yr}^{-1})} = 4.5 \times 10^{-44} \frac{L_{\text{IR}(8-1000)}}{\text{erg s}^{-1}}, \quad (3)$$

where  $L_{\text{IR}(8-1000)}$  is approximately the total luminosity between  $8 \mu\text{m}$  and  $1000 \mu\text{m}$ . This estimation is within  $\sim 30\%$  to other published calibrations. We derived the ratio between  $L_{\text{FIR}(40-120)}$  and  $L_{\text{IR}(8-1000)}$  by computing these two quantities on model spectral energy distributions of six nearby normal and starburst galaxies (Silva et al. 1998), using their original definitions over the *Infrared Astronomical Satellite* (IRAS) bands (see the summary in Sanders & Mirabel 1996). The  $L_{\text{IR}(8-1000)}$  to  $L_{\text{FIR}(40-120)}$  ratio has a range of 1.71–2.32, with a weak anti-correlation between the ratio and IR luminosity and a mean of 2.05. This mean ratio is slightly higher than that used in Yun et al. (2001) of 1.5, which is based on measurements in luminous IRAS galaxies and starburst galaxies (Sanders et al. 1991; Meurer et al. 1999; Calzetti et al. 2000), but is closer to the values in nearby normal spiral galaxies and low luminosity starbursts ( $\sim 2$  for M 51 and M100, and 2.3 for M 82, based on the Silva et al. templates). Using this value, we derived the SFRs listed in Table 2, which are consistent with normal galaxies or low-luminosity starbursts.

#### 3.3.2. UV SFR

The  $i_{775}$  and  $V_{606}$  bands correspond to rest-frame UV, and can be used to calculate SFRs, *uncorrected for extinction*

TABLE 2  
STAR FORMATION RATES DERIVED WITH VARIOUS FLUXES

	Radio		Optical	
	Small aperture	Large aperture	$i_{775}$	$z_{850}$
SFRs( $M_{\odot} \text{ yr}^{-1}$ )	$6.0 \pm 11.0$	$25.7 \pm 18.8$	4.92	5.14

(Madau et al. 1998), with

$$\text{SFR}(M_{\odot} \text{ yr}^{-1}) = \frac{L_{\text{UV}}(\text{ergs s}^{-1} \text{ Hz}^{-1})}{C}, \quad (4)$$

where  $L_{\text{UV}}$  is the UV luminosity density at the same redshift of 3.8, and  $C$  is  $8.0 \times 10^{27}$  and  $7.9 \times 10^{27}$  at  $1500\text{\AA}$  and  $2800\text{\AA}$ , respectively. We list in Table 2 the mean UV SFRs of the  $B$ -dropouts with radio fluxes  $< 100 \mu\text{Jy}$ . The uncorrected SFRs derived from  $i_{775}$  and  $V_{606}$  are remarkably similar to each other as well as to that derived from the radio stacking analyses, indicating very little extinction in the observed rest-frame UV emission.

#### 4. RESULT AND DISCUSSION

##### 4.1. Dust extinction in $z \sim 4$ LBGs

In Figure 2, we plot the  $z_{850}$  magnitudes versus the small-aperture radio fluxes and the corresponding SFRs of all the  $B$ -dropouts in the two fields, with the red points indicating the mean ( $< 100 \mu\text{Jy}$  sources). As can be seen in the figure and Table 2, the *average* SFRs deduced from the radio and the rest-frame UV are consistent within measurement uncertainties. The relatively small SFR derived from the radio flux suggests little extinction in the  $z \sim 4$  LBGs. Unfortunately, although this is by far the deepest radio stacking on  $z \sim 4$  LBGs ( $\sim 3 \times$  deeper than that in Carilli et al. 2008), the error in the stacked radio flux is still too large to pin down the extinction correction. An extinction correction of  $> 6$  is ruled out at  $2.2 \sigma$  and an extinction correction of  $> 4$  is ruled out at  $1.3 \sigma$ . Bouwens et al. (2009) derived extinction corrections of  $\sim 3-6$  for  $z \sim 4$  LBGs based on their UV continuum slopes. Our result slightly favors a lower value and is marginally ( $\sim 2 \sigma$ ) consistent with the result of Bouwens et al. (2009).

We note that an even stricter upper limit on the radio SFR can be placed if any of the following is true: (1) the radio—FIR correlation  $q$  factor exhibits a decline with redshift (see Section 4.3); or (2) the conversion from  $L_{\text{FIR}(40-120)}$  to  $L_{\text{IR}(8-1000)}$  is overestimated (see Section 3.3.1); or (3) there is AGN contribution in our radio SFR (see Section 4.2). The combined effect of all the above may not be negligible and can make the extinction correction for  $z \sim 4$  LBGs even lower. However, this remains to be tested by future observations.

Carilli et al. (2008) found a low extinction correction of 1.8 on  $z \sim 3$  LBGs. On the other hand, on  $z \sim 4$  LBGs, they had a  $2 \sigma$  detection of  $0.83 \pm 0.42 \mu\text{Jy}$  on 1447  $B$ -dropouts, which also suggests a low extinction correction. This radio flux is much higher than ours ( $0.08 \pm 0.15 \mu\text{Jy}$ ) but their ground-based  $V$ -band limiting magnitude is also much shallower than ours (by  $\sim 2$  mag). In other words, we are probing different LBG luminosities. Comparing our  $z \sim 4$  result with the  $z \sim 4$  result in Carilli et al. (2008) is therefore not straightforward.

##### 4.2. AGN contamination

To avoid AGN contamination, a flux cut of  $< 100 \mu\text{Jy}$  was set and eight sources were rejected (one in the north and seven in the south). If these sources comprise *all* the AGNs in our

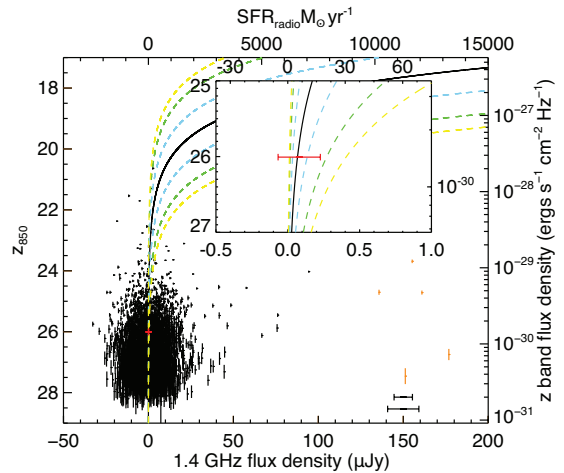


FIG. 2.— *HST*  $z_{850}$  magnitude vs. 1.4 GHz VLA flux of the  $\sim 3500$   $B$ -dropouts in the GOODS fields. Orange symbols indicate objects not included in our stacking analyses. The radio fluxes are measured with small apertures with radii equal to the beam FWHMs ( $\sim 11$  kpc at  $z = 4$ ). The  $z_{850}$  uncertainty of each data point is indicated with vertical bars. The radio uncertainties, which depend on the locations on the maps, are not shown to avoid confusion. Instead, we plot the typical radio flux uncertainties for galaxies close to the center of the 2 fields at the lower-right corner for reference (upper: North, lower: South). The inferred SFR corresponding to the measured flux density at 1.4 GHz (see text for details) is shown on the upper x-axis. The average of all the *black* data points are shown with the red symbols, with the radio uncertainties estimated from the MonteCarlo simulation. The black curves indicate the locus of equal SFR deduced from the  $z_{850}$  and the radio. The color coded curves, from left to right, indicate 1/6, 1/4, 1/2, 2, 4, and 6 times dust corrections from the UV to radio SFR. A blow up to the stacked data point is shown as an insert.

sample, our sample would have a very low AGN fraction of  $\sim 0.2\%$ . For comparison, the AGN fraction in LBGs at  $z \sim 3$  was estimated to be  $\sim 3\%$ , based on optical spectroscopy (Shapley et al. 2003). This difference could be due to the fact that our LBGs are much less luminous than those in the spectroscopic sample.

It is possible to roughly separate AGNs and star forming galaxies based on the radio power. In the local radio luminosity function (e.g., Mauch & Sadler 2007), the 1.4 GHz power that divides AGNs and starbursts is  $\sim 10^{23} \text{ W Hz}^{-1}$ . Cowie et al. (2004) show that this AGN/starburst division increases to  $\sim 10^{24} \text{ W Hz}^{-1}$  at  $z \sim 1$ . This power corresponds to  $\sim 10 \mu\text{Jy}$  for  $z = 4$ . However, the increasing trend observed by Cowie et al. (2004) can continue to  $z \gg 1$ , moving the AGN/starburst division to a radio flux greater than  $10 \mu\text{Jy}$ . Furthermore, high-redshift flat-spectrum radio sources (presumably AGNs) have a more negative  $K$ -correction than that of steep-spectrum sources (starbursts). This also increases the apparent flux division between AGNs and starbursts at observed-frame 1.4 GHz (by roughly a factor of 2). We thus expect sources below our  $100 \mu\text{Jy}$  cut to be dominated by star forming galaxies.

It is interesting to test what happens if we assume that  $> 50 \mu\text{Jy}$  sources are also AGNs and remove them from the stacking analyses. To do this, we rejected 13 sources that are brighter than  $50 \mu\text{Jy}$  and introduced the same  $50 \mu\text{Jy}$  cut in the Monte Carlo simulation. We found a stacked flux of  $0.05 \pm 0.14 \mu\text{Jy}$ , corresponding to a mean SFR of  $3.8 \pm 10.5 M_{\odot} \text{ yr}^{-1}$ . The stacked flux decreases further if we keep lowering the flux cut but the change is well within the noise. Nevertheless, it is obvious that we will get a lower mean SFR if we assume more AGN contribution. Although we are limited by noise here, our conclusions that  $z \sim 4$  LBGs have low SFRs

and the mean extinction correction seems to be lower than 5 are thus still valid.

#### 4.3. The Radio—FIR Correlation

Carilli et al. (2008) discussed the use of the local radio—FIR correlation to derive SFRs of high-redshift galaxies. They mentioned several possibilities that this correlation may be different at high redshift. Indeed, a weak evolution has been suggested by recent studies (Sargent et al. 2010; Ivison et al. 2010a,b). However, as mentioned in Section 3.3.1, even if we extrapolate the evolution based on a declining  $q$  (Ivison et al. 2010b) and adopt a  $L_{\text{IR}(8-1000)}$  to  $L_{\text{FIR}(40-120)}$  ratio that is 25% lower, our main conclusions would not change and this would make the SFR of the LBGs even lower. Furthermore, the local radio—FIR correlation is only used to calibrate the relation between SFR and radio power. Even if there is an evolution in the radio—FIR correlation at high redshift, we cannot be certain that the evolution arises from the radio part of the correlation and affects the radio—SFR relation. In short, we see neither evidence nor strong argument that the radio SFR is significantly biased by the assumption of the local radio—FIR correlation.

#### 4.4. Implications for SMGs

The relatively low dust correction and SFRs imply that  $z \sim 4$  LBGs in general do not have extreme star formation activities enshrouded in dust, unlike that in SMGs. If the total SFR of our  $z \sim 4$  LBGs is only contributed by SMGs with SFR of  $1000 M_{\odot} \text{ yr}^{-1}$  and if other non-SMG LBGs have no star forming activities, then there can be no more than  $21 \pm 39$  SMGs in our LBG sample. In comparison, the source counts at  $850 \mu\text{m}$  (Coppin et al. 2006) suggest  $\sim 350$  SMGs in a field of the combined GOODS size, with  $S_{850} > 1.4$  mJy and a mean SFR of  $1000 M_{\odot} \text{ yr}^{-1}$ . This means that even if the total SFR of our LBG sample is dominated by  $z \sim 4$  SMGs, they can only account for  $< 10\%$  of the entire SMG population at  $S_{850} > 1.4$  mJy. This implies that either LBGs and SMGs have little overlap at  $z \sim 4$  or most SMGs are at  $z \ll 4$ . We note that previous studies in the submillimeter showed that LBGs are in general not SMGs (Chapman et al. 2000; Peacock et al. 2000; Webb et al. 2003), and that most SMGs are at  $z < 3.5$  (Chapman et al. 2003, 2005). Our results are consistent with these.

Another scenario related to SMGs worth investigating is dust-hidden companions sitting close to the LBGs. An example of this is the  $z = 4.5$  SMG in Capak et al. (2008). This galaxy is independently selected as an LBG, and has an ultraluminous dusty component showing up at  $> 3.6 \mu\text{m}$  next to its rest-frame UV emission. To know whether similar systems

are common at  $z \sim 4$ , we performed the same radio stacking using the large apertures with radii twice the beam FWHM ( $\sim 22$  kpc at  $z = 4$ ) to measure the radio fluxes. As shown in Figure 3 and Table 2, the radio SFR is slightly higher but still consistent with the UV SFR, implying that there is no statistically significant excess of dust-hidden star-forming components close to LBGs.

## 5. SUMMARY

We employed radio stacking analyses on  $\sim 3500$  LBGs at  $z \sim 4$  in the GOODS-N and GOODS-S fields. The mean radio flux was converted to FIR luminosity via the well-known radio—FIR correlation, and then converted to an intrinsic SFR, which is  $6 \pm 11 M_{\odot} \text{ yr}^{-1}$ . By comparing with SFRs esti-

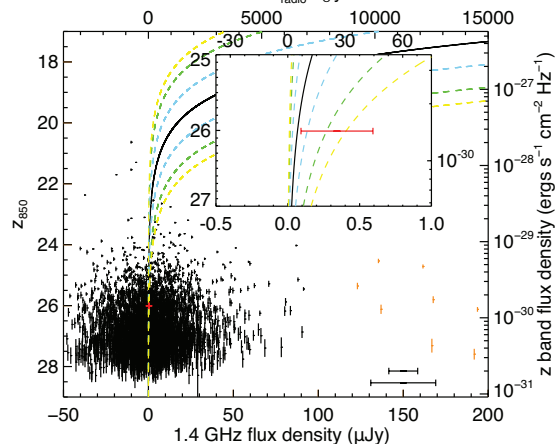


FIG. 3.— Same as Figure 2, but the radio fluxes are measured with apertures of radii twice the beam FWHM ( $\sim 22$  kpc at  $z = 4$ ).

mated from rest-frame UV, we found a maximum UV extinction correction of  $\sim 6$ . This is roughly consistent with that derived from UV continuum slopes by Bouwens et al. (2009) with a very similar sample. The low extinction correction confirms that  $z \sim 4$  LBGs are in general not SMGs. We also investigated the possibility of finding dust-hidden companions close to the LBGs at  $z \sim 4$ . The stacked radio flux within  $\sim 22$  kpc to the LBGs implies a mean SFR that is still consistent with the UV inferred SFR, which suggests no statistically significant excess of dust-hidden star-forming components close to LBGs.

We thank the referee for providing comments that improve this paper. W.-H.W. and I.-T.H. acknowledge a grant from the National Science Council of Taiwan (98-2112-M-001-003-MY2).

## REFERENCES

- Beckwith, S. V. W., et al 2006, *AJ*, 132, 1729  
 Bertin, E., & Arnouts, S. 1996, *A&AS*, 117, 393  
 Bouwens, R. J., Illingworth, G., D., Franx, M., & Ford, H. 2007, *ApJ*, 670, 928  
 Bouwens, R. J. et al. 2009, *ApJ*, 705, 936  
 Calzetti, D., Armus, L., Bohlin, R. C., Kinney, A. L., Koornneef, J., & Storchi-Bergmann, T. 2000, *ApJ*, 533, 682  
 Capak, P. et al. 2008, *ApJ*, 681, L53  
 Carilli, C. L. et al. 2008, *ApJ*, 689, 883  
 Chapman, S. C. et al 2000, *MNRAS*, 319, 318  
 Chapman, S. C., Blain, A. W., Ivison, R. J., & Smail, I. R. 2003, *Nature*, 422, 695  
 Chapman, S. C., Blain, A. W., Smail, I., & Ivison, R. J. 2005, *ApJ*, 622, 772  
 Condon J. J., 1992, *ARA&A*, 30, 575  
 Coppin, K. et al. 2006, *MNRAS*, 372, 1621  
 Cortese, L. et al. 2006, *ApJ*, 637, 242  
 Cowie, L. L., Barger, A. J., Fomalont, E. B., & Capak, P. 2004, *ApJ*, 603, L69  
 Cowie, L. L., Lilly, S. J., Gardner, J. & Mclean, I. S. 1988, *ApJ*, 332, L29  
 Devlin, M. J. et al. 2009, *Nature*, 458, 737  
 Giavalisco, M. 2002, *ARA&A*, 40, 579  
 Giavalisco, M., et al. 2004, *ApJ*, 600, L93  
 Helou, G., Soifer, B. T. & Rowan-Robinson, M. 1985, *ApJ*, 298, L7  
 Howell, J. H. et al. 2010, *ApJ*, 715, 572  
 Ivison, R. J. et al. 2010a, *A&A*, 518, 31  
 Ivison, R. J. et al. 2010b, *MNRAS*, 402, 245

- Kennicutt, Jr., R. C. 1998, *ARA&A*, 36, 189  
Lilly, S. J., Cowie, L. L. & Gardner, J. 1991, *ApJ*, 369, L79  
Marsden, G. et al. 2009, *ApJ*, 707, 1729  
Mauch, T. & Sadler, E. M. 2007, *MNRAS*, 375, 931  
Madau, P., Pozzetti, L. & Dickinson, M. 1998, *ApJ*, 498, 106  
Meurer, G. R., Heckman, T. M. & Calzetti, D. 1999, *ApJ*, 521, 64  
Miller, N. A., Fomalont, E. B., Kellermann, K. I., Mainieri, V., Norman, C.,  
Padovani, P., Rosati, P., & Tozzi, P. 2008, *ApJS*, 179, 114  
Morrison, G. E., Owen, F. N., Dickinson, M., Ivison, R. J., & Ibar, E. 2010,  
*ApJS*, 188, 178  
Pannella, M. et al. 2009, *ApJ*, 698, L116  
Peacock, J. A. et al. 2000, *MNRAS*, 318, 535  
Perera, T. A. et al. 2008, *MNRAS*, 391, 1227  
Reddy, N. A. & Steidel, C. C. 2004, *ApJ*, 603, L13  
Sanders, D. B. & Mirabel, I. F. 1996, *ARA&A*, 34, 749  
Sanders, D. B., Scoville, N. Z., & Soifer, B. T. 1991, *ApJ*, 370, 158  
Sargent, M. T. et al. 2010, *ApJ*, 714, L190  
Shapley, A., Steidel, C., Pettini, M., & Adelberger, K. 2003, *ApJ*, 588, 65  
Silva, L., Granato, G. L., Bressan, A. & Danese, L. 1998, *ApJ*, 509, 103  
Songaila, A., Cowie, L. L. & Lilly, S. J. 1990, *ApJ*, 348, 371  
Steidel, C. C. & Hamilton, D. 1993, *AJ*, 105, 2017  
Steidel, C. C., Pettini, M. & Hamilton, D. 1995, *AJ*, 110, 2519  
Wang, W.-H., Cowie, L. L. & Barger, A. J. 2004, *ApJ*, 613, 655  
Wang, W.-H., Cowie, L. L. & Barger, A. J. 2006, *ApJ*, 647, 74  
Webb, T. M. et al. 2003, *ApJ*, 582, 6  
Weiß, A. et al. 2009, *ApJ*, 707, 1201  
Yun, M. S., Reddy, N. A., & Condon, J. J. 2001, *ApJ*, 554, 803